Calcium currents and transients in co-cultured contracting normal and Duchenne muscular dystrophy human myotubes

Nathalie Imbert, Clarisse Vandebrouck, Gérard Duport, Guy Raymond, Abdul A. Hassoni, Bruno Constantin, Michael J. Cullen, Christian Cognard

Calcium currents and transients in co-cultured contracting normal and Duchenne muscular dystrophy human myotubes

Nathalie Imbert, Clarisse Vandebrouck, Gérard Duport*, Guy Raymond, Abdul A. Hassoni†, Bruno Constantin, Michael J. Cullen‡ and Christian Cognard

*Laboratoire de Biomembranes et Signalisation Cellulaire, UMR CNRS/Université de Poitiers 6558, 86022 Poitiers Cedex, France, *Service de Chirurgie Générale, Centre Hospitalier Universitaire, 86024 Poitiers Cedex, France, †Division of Pharmacology, Kings College London, St Thomas's Hospital Campus, London SE1 7EH, UK and ‡Department of Neurobiology, The Medical School, University of Newcastle, Framlington Place, Newcastle upon Tyne NE2 4HH, UK*

(Received 4 October 2000; accepted after revision 7 March 2001)

1. The goal of the present study was to investigate differences in calcium movements between normal and Duchenne muscular dystrophy (DMD) human contracting myotubes co-cultured with explants of rat spinal cord with attached dorsal root ganglia. Membrane potential, variations of intracellular calcium concentration and T- and L-type calcium currents were recorded. Further, a descriptive and quantitative study by electron microscopy of the ultrastructure of the co-cultures was carried out.

2. The resting membrane potential was slightly less negative in DMD (-61.4 ± 1.1 mV) than in normal myotubes (-65.5 ± 0.9 mV). Both types of myotube displayed spontaneous action potentials (mean firing frequency, 0.42 and 0.16 Hz, respectively), which triggered spontaneous calcium transients measured with Indo-1.

3. The time integral under the spontaneous Ca^{2+} transients was significantly greater in DMD myotubes (97 ± 8 nM s) than in normal myotubes (67 ± 13 nM s).

4. The L- and T-type current densities estimated from patch-clamp recordings were smaller in DMD cells (2.0 ± 0.5 and 0.90 ± 0.19 pA pF^{-1}, respectively) than in normal cells (3.9 ± 0.7 and 1.39 ± 0.30 pA pF^{-1}, respectively).

5. The voltage-dependent inactivation relationships revealed a shift in the conditioning potential at which inactivation is half-maximal ($V_{h,0.5}$) of the T- and L-type currents towards less negative potentials, from -72.1 ± 0.7 and -53.7 ± 1.5 mV in normal cells to -61.9 ± 1.4 and -29.2 ± 1.4 mV in DMD cells, respectively.

6. Both descriptive and quantitative studies by electron microscopy suggested a more advanced development of DMD myotubes as compared to normal ones. This conclusion was supported by the significantly larger capacitance of the DMD myotubes (408 ± 45 pF) than of the normal myotubes (299 ± 34 pF) of the same apparent size.

7. Taken together, these results show that differences in T- and L-type calcium currents between normal and DMD myotubes cannot simply explain all observed alterations in calcium homeostasis in DMD myotubes, thus suggesting that other transmembrane calcium transport mechanisms must also be altered in DMD myotubes compared with normal myotubes.

Duchenne muscular dystrophy (DMD) is caused by mutations in the DMD gene (Hoffman *et al.* 1987), which controls the expression of dystrophin. This protein, normally localized beneath the sarcolemma in normal muscle, is absent in muscle from DMD patients (Bonilla *et al.* 1988). DMD is also characterized by an abnormally high concentration of intracellular ionized calcium (Bodensteiner & Engel, 1978), which is thought to contribute to the final muscle necrosis. This resting calcium accumulation in DMD cells was also observed *in*

vitro provided the human muscle cells were co-cultured with neurones, that is in more mature DMD myotubes at the stage at which they begin to contract (Rivet-Bastide *et al.* 1993; Imbert *et al.* 1995). By contrast no elevation of resting calcium level has been found in aneural cultured myotubes from DMD muscle (Rivet-Bastide *et al.* 1993; Pressmar *et al.* 1994). Since one of the functions of calcium channel molecules is to transfer calcium ions into the cells, this process could be one of the potential candidates for contributing to the calcium entry and accumulation in DMD cells. *In vitro* studies on aneurally cultured cells have shown the existence of at least two types of voltage-dependent calcium current (T and L); their characteristics have been extensively studied in normal (Rivet *et al.* 1990, 1992; Garcia *et al.* 1992; Sipos *et al.* 1997; Morill *et al.* 1998; Harasztosi *et al.* 1999) and DMD muscle cells (Rivet *et al.* 1990), but no obvious differences in the voltage dependence and kinetics of these calcium currents have been observed, as expected from cells in which the resting intracellular calcium concentration remained similar. Consequently, in order to address a possible involvement of such calcium channels in the detected intracellular calcium concentration elevation, investigations in co-cultured human muscle cells were essential despite the low availability of DMD biopsies. In contrast to hypokalaemic periodic paralysis or to malignant hyperthermia susceptibility, in which mutations of the $\alpha 1$ subunit of the dihydropyridine-sensitive calcium channel are directly related to the diseases (Jurkat-Rott *et al.* 1994; Ptacek *et al.* 1994; Sipos *et al.* 1995; Monnier *et al.* 1997), the calcium deregulation aspect of the DMD pathological phenotype possibly results from an indirect alteration, through the absence of dystrophin, of the regulation of several calcium transfer mechanisms. The purpose of the present study was to compare electrical and calcium homeostasis properties of normal and DMD co-cultured human myotubes, with a particular interest in calcium currents. Further, electron microscopy, focused on ultrastructural elements involved in calcium homeostasis, excitation–contraction coupling or contractility, provided additional data on the potential involvement of calcium channels in the calcium overload observed in co-cultured DMD cells.

METHODS

Culture and co-culture of human skeletal muscle cells

As previously described (Rivet *et al.* 1990), primary cultures of human skeletal muscle cells were initiated from satellite cells of muscle samples obtained during orthopaedic surgery (with the agreement of the Comité pour l'Ethique Médicale du Centre Hospitalier Régional de Poitiers and in accordance with French institutional guidelines) from patients without a neuromuscular disorder ($n = 35$) and DMD patients ($n = 16$). Informed consent was given in writing before surgery by the subject or his relatives, and all work conformed with the Declaration of Helsinki. Muscle biopsies were trimmed of fat and connective tissue, then minced into 1 mm^3 fragments in calcium- and magnesium-free saline solution (Spinner medium containing (mM): 8 NaH_2PO_4; 22.6 $NaHCO_3$; 116 NaCl; 5.3 KCl; and 5.6 glucose; pH 7.4). Satellite cells were obtained by enzymatic dissociation (at 37 °C) with Spinner medium containing 0.2 % (w/v) trypsin (Seromed, Biochrom KG, Berlin, Germany). The supernatants of successive dissociations (4 or 5) were centrifuged (200 *g* for 5 min) and the pellet resuspended in growth medium containing Ham's F10 (Gibco BRL, Life Technologies, Cergy Pontoise, France) supplemented with 10 % fetal calf serum (Boehringer Mannheim, Meylan, France) and 10 % heat-inactivated horse serum (Gibco BRL). The number of satellite cells collected and used to initiate the cultures was a central problem as this number depends on several parameters and could effect the maturation rate. These parameters include the size of the biopsy, the type of donor (satellite cell number is more elevated in DMD, see Maier & Bornemann, 1999), the age of donor (the number decreases with age), and the number of dissociation enzyme cycles and their efficiency (the global output could be decreased by the presence of remaining connective or fatty tissue). To overcome this problem the cultures were always initiated after cell counting and a dilution to obtain the same final seeding density (see below), in order to have comparable starting culture conditions, not only between normal and DMD cultures but also between different cultures of cells of the same origin. Thus, after filtration of the cell suspension through nylon netting (pore size, 25 μm), the satellite cells were counted and then seeded (final seeding density of 200 000 cells ml^{-1}) in 35 mm Petri dishes (Nunc Delta, Nunc, Raskilde, Denmark; 2 ml per dish). Following 8–15 days of proliferation (37 °C, 5 % CO_2, water-saturated air) at the end of which the cells align, the growth medium was replaced by one containing F14 medium (Gibco BRL) supplemented with 10 % fetal bovine serum (Sigma, St Louis, MO, USA) and 10 μg ml^{-1} insulin (Sigma) to induce the fusion of myoblasts into myotubes. Following the start of fusion (24 h), whole transverse slices of 13-day-old rat embryo spinal cord with attached dorsal root ganglia were dissected in Hanks' balanced salt solution (mM): 1.26 $CaCl_2$; 5.36 KCl; 0.44 KH_2PO_4; 0.81 $MgSO_4$; 136.9 NaCl; 4.2 $NaHCO_3$; 0.34 Na_2HPO_4 $7H_2O$; and 33.3 glucose. Embryos were rapidly removed from rats killed by cervical dislocation and decapited. Four or five explants per Petri dish were placed on the muscle monolayer cultures. Co-cultures were maintained in the same medium as described above. All culture media contained 1 % v/v antibiotics (penicillin-G, 100 U ml^{-1}; streptomycin, 50 μg ml^{-1}) and were renewed at 2–3 day intervals throughout the culture.

Cell selection for patch clamping, calcium measurement and electron microscopy

The electrophysiological study began as soon as spontaneous contractions had been detected in Petri dishes, and were conducted between 6 and 14 days after addition of neural explants (15–30 days in culture). Around 2 weeks later, the myotubes became too large for the patch-clamp technique. The tested myotubes were selected by eye, with the help of a micrometer eye-piece, on the basis of their small size, non-branching geometry and thin cylindrical aspect with fusiform ends. The selected myotubes had a diameter (width) of 14–16 μm and a length of 240–260 μm. More selective criteria were not possible. In the case of the width the useable limit of the optical resolution was 1–2 μm (×40 objective lens) and in the case of the length the range was chosen in order to keep a realistic size compatible with the patch-clamp technique, and also to increase the chance of finding a sufficient number of myotubes considering the limited availability of the DMD cultures. The same selection criteria were used for calcium measurement experiments. In contrast, since electron microscopy (EM) precluded selection by the same criteria as in the classical phase contrast microscopy used in the other experiments (see below), the cell dishes used were only selected on the basis of age. The processes of fixation, embedding and sectioning may have induced some alteration in the size and shape of the fixed myotubes (as compared to living cells). Moreover the plane of the section did not always correspond to that of the myotube longitudinal axis. The size of the profile viewed, therefore, was smaller than the cell itself and,

for example, only one nucleus might be included in the section when in fact several were present in the myotube. Thus, it was generally not possible to have a global view of an entire cell in the EM. Consequently the only valid approach was to make a selection based on cultures of the same age in a qualitative and quantitative study. Thus, for EM the co-cultured cells were 13–14 days old after addition of neural explants, i.e. 26–27 days in culture.

Calcium activity recording

Resting calcium level and spontaneous calcium variations were followed using a pulsed argon laser cytometer (ACAS 570 Meridian) and the fluorescent dye Indo-1 (Indo-1 AM, Molecular Probes, Calbiochem or Sigma). Details of the technique have been reported elsewhere (Rivet-Bastide *et al.* 1993). Cells were loaded with Indo-1 AM (the permeant form of Indo-1) at 3 μM for 60 min in the dark at room temperature, then incubated in control solution for 10 min at 37 °C to obtain a large de-esterification of the acetoxymethylester probe. The experiments were performed at room temperature. The culture medium was replaced before each experiment by a saline bath solution containing (mM): 130 NaCl; 5.4 KCl; 2.5 $CaCl_2$; 0.8 $MgCl_2$; 5.6 glucose; and 10 Hepes; pH 7.4 with Tris base. Intracellular calcium level variations were measured from a fixed small volume of the cell, corresponding to the excitation laser beam impact, and were estimated as the ratio of the 405 nm to the 485 nm emissions of the Ca^{2+}-bound to the Ca^{2+}-free forms of the dye, respectively. Then, cytosolic free calcium activities were calculated from the Grynkiewicz equation: $[Ca^{2+}]_i = K_d\beta((R - R_{min})/(R_{max} - R))$ taking 250 nM for K_d (Grynkiewicz *et al.* 1985). R is the ratio of the 405 nm to the 485 nm emissions as defined above and R_{min} and R_{max} are the minimum and maximum values, respectively, reached by R. The β constant, R_{min} and R_{max} values were determined *in vivo* at the end of the experiments by a calibration method described previously (Imbert *et al.* 1995). The parameters differed from cell to cell regardless of the cell type. In order to compute the resting calcium concentration in the two types of cell the parameters were determined in two sampled groups. The mean values of the β constant were 2.01 ± 0.16 ($n = 7$; with a minimum value of 1.62 and a maximum value of 2.53) and 2.20 ± 0.06 ($n = 36$; with a minimum value of 1.49 and a maximum value of 2.78) for normal and DMD myotubes, respectively. The mean values of R_{min} were 0.43 ± 0.03 ($n = 7$; with a minimum value of 0.35 and a maximum value of 0.58) and 0.53 ± 0.01 ($n = 36$; with a minimum value of 0.42 and a maximum value of 0.75) for normal and DMD myotubes, respectively. The mean values of R_{max} were 1.64 ± 0.14 ($n = 7$; with a minimum value of 1.19 and a maximum value of 1.98) and 1.89 ± 0.06 ($n = 36$; with a minimum value of 1.32 and a maximum value of 2.29) for normal and DMD myotubes, respectively.

Membrane current recording

Calcium currents were recorded at room temperature (18–20 °C) from co-cultured myotubes with the whole-cell patch-clamp technique (Hamill *et al.* 1981). Glass micropipettes (2–5 MΩ) were connected to the headstage of the patch-clamp amplifier (RK300, Bio-logic, Claix, France) driven by a PC microcomputer equipped with a TM40 Labmaster A/D conversion board (Scientific Solutions, Solon, OH, USA). Membrane voltage clamping, data acquisition and analysis were performed by means of the pCLAMP software package (Axon Instruments, Foster City, CA, USA) and data graphics through Fig.P software (Fig.P Corp., Biosoft, Cambridge, UK). Unless stated otherwise, the time interval between each pulse was 30 s. Leak currents were estimated by linear extrapolation of currents induced by small depolarizations (assumed to be ohmic) and then subtracted from whole-cell currents. Depolarizations were applied from an appropriate holding potential (V_h), specified for each experiment. The inward current amplitude was measured as the difference between the peak amplitude and zero current levels after leakage subtraction. For the drawing of current–voltage (I–V) curves, the current density was calculated by normalizing the ionic current amplitude to the membrane capacity (C_m). The series resistance was measured in the two groups of myotubes and its mean value was 7.0 ± 1.0 MΩ ($n = 16$) with a maximum value of 16.8 MΩ and 5.8 ± 0.7 MΩ ($n = 26$) with a maximum value of 13 MΩ in normal myotubes and DMD myotubes, respectively. These series resistances were approximately 80 % compensated through the built-in device of the amplifier. Thus, in the present experiments, the remaining series resistances were around 1.40 MΩ (normal) and 1.16 MΩ (DMD) with maximum remaining values of 3.36 and 2.60 MΩ in normal and DMD myotubes, respectively. Given a mean current amplitude (see Results) of 1.2 nA (normal) or 0.8 nA (DMD), the mean voltage drop errors, caused by current flowing through the series resistances, were 1.7 and 1.0 mV in normal and DMD myotubes, respectively. The corresponding maximum values were 6.0 and 5.7 mV. The internal and external media were designed in order to isolate calcium currents. Pipettes were filled with an internal medium containing (mM): 145 CsCl; 1 $MgCl_2$; 0.005 $CaCl_2$; 1 EGTA; 2 ATP disodium salt; and 5.6 glucose; pH 7.2 with Tris base. Just before each experiment, the culture medium was changed for an external solution (test solution) containing (mM): 135 TEA-Cl; 2.5 $CaCl_2$; 0.08 $MgCl_2$; 5.6 glucose; and 10 Hepes; pH 7.4 with TEA-OH. To abolish the sodium current, Na^+ ions were absent from the external medium, being replaced with equimolar quantities of TEA. Internal Cs^+ ions and external TEA-Cl were used to block or minimize outward currents. During experiments, exchanges of external solutions were performed by means of a micro-superfusion device developed in this laboratory. Nifedipine (5 μM) was added to the external medium from a stock solution in DMSO (Sigma). As DMSO was used as the solvent of nifedipine, it was also added to the control solution at a final concentration corresponding to that in the nifedipine-containing solution.

Membrane potential recording

Resting membrane potential (V_m) was recorded with the whole-cell patch-clamp technique using the current-clamp mode (current was clamped to zero). In this case, pipettes were filled with an internal medium containing (mM): 1 $MgCl_2$; 0.37 $CaCl_2$; 1 EGTA; 1.3 NaCl; 155 potassium acetate; 9 sodium acetate; and 2 ATP disodium salt; pH 7.2 with KOH. The external medium was composed of (mM): 1.1 $MgCl_2$; 2.2 $CaCl_2$; 5.6 glucose; 10 Hepes; 150 NaCl; and 4 KCl; pH 7.4 with KOH.

Electron microscopy

As stated in the cell selection section, a quantitative investigation was carried out in addition to the descriptive study, and the rationale for this is explained and discussed in the corresponding section of the Results. Cultured cells were fixed at 4 °C (pH 7.4) for 1 h in 2 % glutaraldehyde in 0.1 M cacodylate buffer. Preparations were washed in 0.1 M cacodylate buffer at 4 °C (pH 7.4) for 1 h, then postfixed in 1 % osmium tetroxide at room temperature for 1 h and embedded in Epon. The bases of the resin blocks were then stained with 1 % toluidine blue, which allowed the cultures to be viewed by bright field microscopy through the resin. Areas containing well-defined myotubes were then cut out and re-mounted on blank blocks ready for sectioning. Thin sections (~80 μm) were cut on a Reichert OMU4 ultramicrotome and collected on cleaned copper grids. They were stained with a saturated solution of uranyl acetate in 30 % methanol followed by 1 % aqueous lead citrate and viewed under a JEOL 1200EX electron microscope.

Statistical analysis

Statistical analysis was performed using GraphPad Prism for Windows (versions 2.00 and 3.00, GraphPad Software, San Diego, CA, USA; www.graphpad.com) according to Student's t test for unpaired data. Results were averaged and are expressed as the mean ± S.E.M.

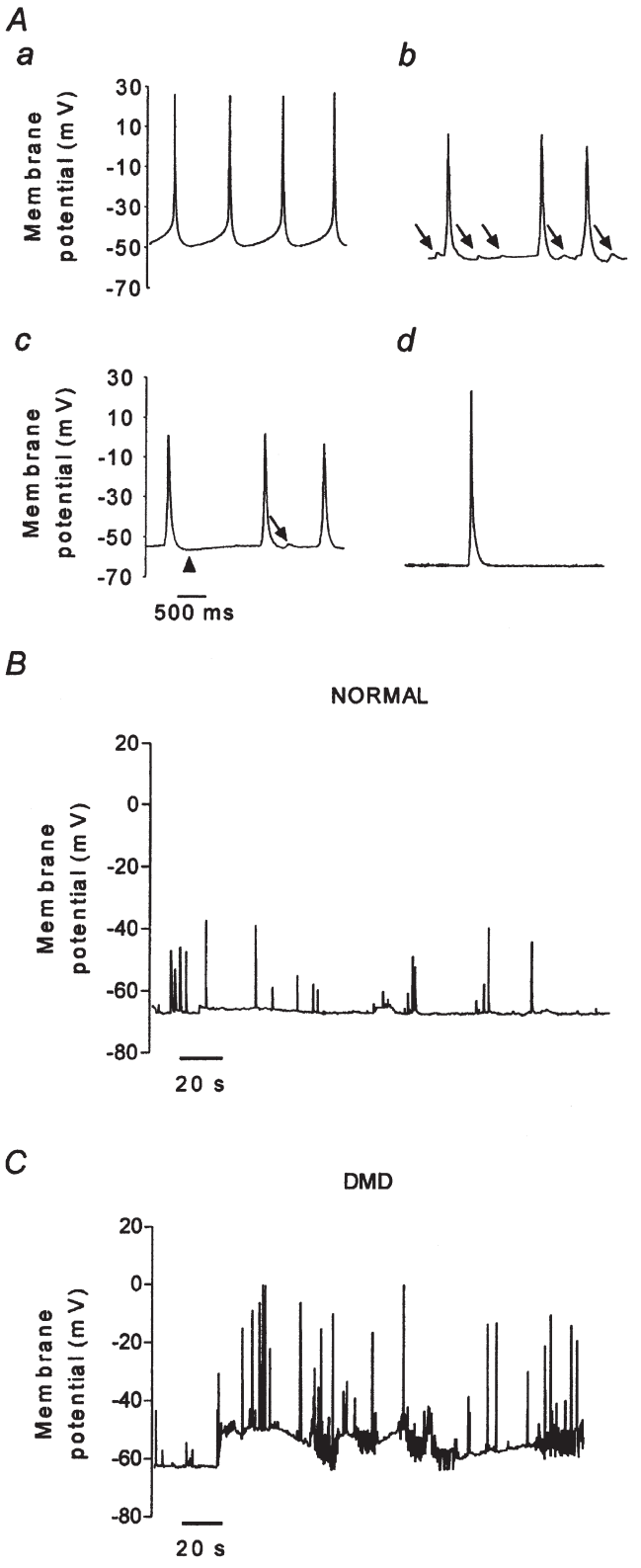

Figure 1. Spontaneous variations of membrane potential in co-cultured normal or DMD muscle cells

A, pacemaker-like activity, aborted APs (arrows) and after-hyperpolarization phase (arrow head) in DMD (*a*,*c*) and normal (*b*,*d*) co-cultured human myotubes. *B* and *C*, global membrane potential variations recorded with a slower time base in normal (*B*) and DMD (*C*) cells.

RESULTS

Spontaneous variations in membrane potential

In contrast to aneurally cultured human skeletal cells, co-cultured cells display spontaneous contractile activity (see Delaporte *et al.* 1986; Kobayashi *et al.* 1987; Saito *et al.* 1990; Imbert *et al.* 1995) a few days after the initiation of the fusion of myoblasts into myotubes. In the present experiments, this contractile activity (visually observed from 6 days after initiation of the fusion process) was accompanied by electrical activity (Fig. 1), i.e. by spontaneous membrane depolarizations. Although a detailed study of this electrical activity was outside the subject of the work reported here, a great variety in time course, shape and amplitude could be observed. Regardless of the type of cell, activity was observed as rare regular pacemaker-like activity (Fig. 1*Aa*) or, in contrast, as action potentials (APs) separated by numerous aborted APs (Fig. 1*Ab*, arrows). The shape of the APs themselves was variable, probably depending on the resting membrane potential and involved ionic mechanisms. Hyperpolarization phases generally followed APs (Fig. 1*Ac*, arrow head) with a slow return to the resting potential. This hyperpolarization phase was absent in highly polarized myotubes (Fig. 1*Ad*). More typical were the long-term variations of the electrical activity, which could be recorded at a lower time resolution. These records revealed 'silent' periods followed by bursts of activity as illustrated in Fig. 1*B* (normal myotubes) and *C* (DMD myotubes). Study of the membrane potential level during resting periods in both cell types showed that DMD myotubes were slightly depolarized as compared to normal cells, with a significant difference ($P = 0.02$) between mean values of V_m (-65.5 ± 0.9 mV ($n = 10$) and -61.4 ± 1.1 mV ($n = 20$) for normal and DMD myotubes, respectively). DMD cells exhibited long periods of depolarization (10–15 mV in amplitude in Fig. 1*C*) from which numerous APs were generated. Regardless of the level of the resting potential, the mean frequency of the AP generation, numbered within 10 or 100 s periods, was 0.42 ± 0.09 Hz in DMD cells ($n = 8$) against 0.16 ± 0.04 Hz in normal cells ($n = 6$). These values were significantly different with $P = 0.03$.

Spontaneous calcium transients

The resting intracellular calcium level of myotubes used in the experiments on calcium level variations depended on the origin (normal or DMD) of the cells since calculation of the corresponding values revealed a significant elevation of the resting calcium concentration in the DMD co-cultured myotubes. The resting $[Ca^{2+}]_i$ was 104 ± 8 nM ($n = 36$) in DMD cells compared with 46 ± 3 nM ($n = 7$) in normal cells. These values are similar to the results reported in two previous papers for the same types of co-culture (Imbert *et al.* 1995; Vandebrouck *et al.* 1999). Regardless of the origin of the biopsies, human co-cultured myotubes also exhibited spontaneous transient

elevations of intracellular calcium level as shown in Fig. 2*A–E*. Such activity appeared to be more frequently observed in DMD myotubes. Given a 25 nM deviation from the resting calcium level as the threshold for considering the variation as a sign of the presence of an activity, a comparative study (within 100 s recording periods) in DMD and normal cells showed that these spontaneous calcium transients were observed in 55% of investigated DMD myotubes ($n = 127$) compared with only 16% of normal ones ($n = 45$). Sometimes the irregular activity in the DMD cells (never seen in normal myotubes) even made difficult the determination of the resting calcium level because of the short period during which the calcium signal remained at its basal level (see the example of Fig. 2*C*). Since the frequency and the amplitude of the calcium transients themselves greatly varied, quantification was required to characterize the calcium transient variations in both types of cell. Computer integration (10 s in duration) of the area delimited by the trace and the straight dotted line fitting the resting level (see Fig. 2*E*) revealed that spontaneous calcium transients were greater in DMD myotubes (97 ± 8 nM s; $n = 50$) than in normal cells that exhibited such activity (67 ± 13 nM s; $n = 7$). Although the technical facilities available in the laboratory did not allow simultaneous recording of calcium transients and membrane potential variations, at least a part of the calcium transients was time related to the membrane potential variations (APs) as judged by the observation of a concomitant contractile activity. Moreover, it can also be considered that the two types of phenomena (APs and calcium transients) are effectively related since the application of tetrodotoxin (not shown) led to the disappearance of these two phenomena as well as of the contractile activity.

Passive membrane properties

Cell capacitance was measured in most of the myotubes selected for the whole-cell voltage-clamp experiments from the capacitive transient elicited by a 10 mV depolarizing step pulse from the holding membrane potential. The selection by eye of myotubes (see Methods) should not result in the introduction of a measurement bias, and similar mean membrane capacity values were expected to be obtained in normal and DMD myotubes since the aim of the cell selection was to work on suitable cells with a similar apparent size, not too big to perform whole-cell patch-clamp experiments. Surprisingly, in spite of a large scattering of the data, DMD co-cultured myotubes displayed a higher mean capacity (408 ± 45 pF; $n = 34$) than the normal cells (299 ± 34 pF; $n = 28$).

Calcium current analysis

Figure 3 shows example recordings of inward calcium currents in normal and DMD co-cultured myotubes (Fig. 3*A*) and corresponding mean peak amplitude I–V curves (Fig. 3*B*). Depolarizing pulses from a V_h of −90 mV induced, in normal and DMD myotubes, the development of two kinds of inward calcium current. Depolarizations

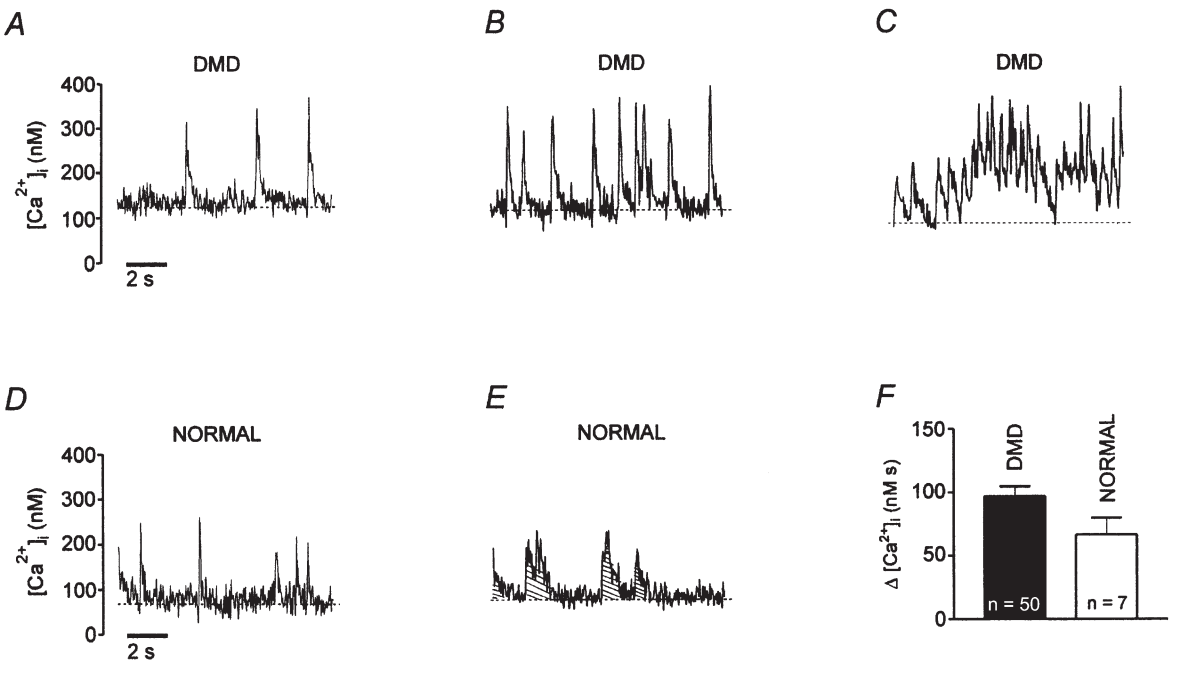

Figure 2. Spontaneous calcium transients in normal and DMD cells

Examples of spontaneous calcium transients in DMD (*A–C*) and normal (*D* and *E*) myotubes. The dotted lines correspond to the basal level of intracellular free calcium concentration in each cell. *F*, the area under each spontaneous calcium transient recording (as shown by the hatched area in *E*) allows quantification of these calcium variations in normal and DMD myotubes. *n* corresponds to the number of tested cells.

Table 1. Kinetics parameters of T- and L-type calcium currents in co-cultured normal and DMD myotubes

	$I_{Ca,T}$		$I_{Ca,L}$	
	Normal	DMD	Normal	DMD
Time to peak (ms)	24 ± 3	33 ± 2*	132 ± 10	212 ± 23**
	$n = 21$	$n = 23$	$n = 26$	$n = 27$
τ activation (ms)	—	—	27 ± 3	49 ± 6**
	—	—	$n = 24$	$n = 25$
τ inactivation (ms)	34 ± 2	37 ± 2	1210 ± 296	1050 ± 240
	$n = 21$	$n = 24$	$n = 26$	$n = 24$

The data are given as means ± S.E.M. Asterisks indicate a difference between the normal and DMD myotubes considered as significant (* $0.01 \leqslant P < 0.05$ and ** $P < 0.01$) using Student's unpaired t test.

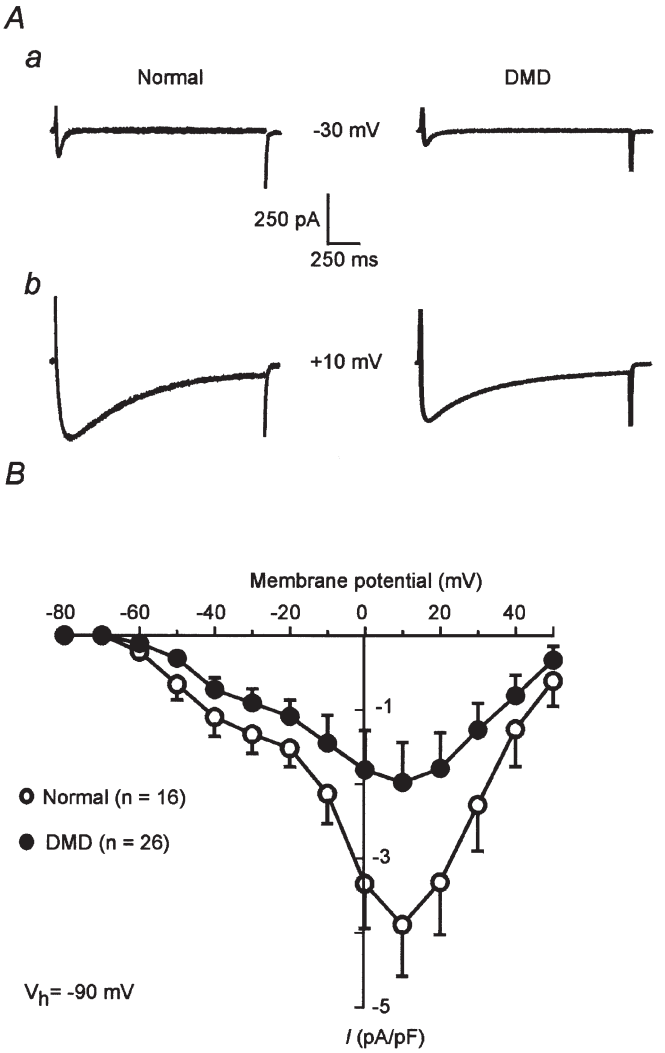

Figure 3. Calcium current recordings and *I–V* curves

A, examples of calcium currents recorded for a depolarization from −90 to −30 mV (*a*) and to +10 mV (*b*) in normal (left) and DMD (right) myotubes. *B*, *I–V* curves obtained in normal (○) and DMD (●) cells. *I* is expressed as the peak current density (pA pF^{-1}). *n* corresponds to the number of tested cells. Values are given as means ± S.E.M.

in the range −60 to −20 mV induced a fast activating and inactivating current as shown for a pulse to −30 mV in Fig. 3*Aa*. An additional inward component with a slow inactivation process progressively developed in both types of myotube from a value of the step potential of around −20 mV. For higher depolarizing steps this calcium current component progressively overlapped the transient one (see traces of Fig. 3*Ab*). The *I–V* curves revealed a threshold potential for the first component of around −60 mV and a maximum amplitude of the slow component for a pulse to +10 mV. The inward current tends to zero at a potential above +50 mV. Clearly these two peaks of the *I–V* curves correspond to two kinds of inward calcium current present in both normal and DMD myotubes. Their properties, described above, are similar in the two types of cell, except for a slowing down of the kinetics in DMD cells, and the amplitudes (current densities), which were greater in normal myotubes.

The kinetics of the currents were compared for the two kinds of muscle (Table 1). The time-to-peak, inactivation and activation time constants were studied at −30 mV for T-type current, $I_{Ca,T}$, and +10 mV for L-type current, $I_{Ca,L}$. The mean values of these parameters were modified in DMD cells, so that the kinetics were slowed down as compared to those in normal cells. Note that the time constants of activation of the fast component of the calcium current were not included in the table because these particular data are questionable. Due to the large size of the cells, the actual value of the potential at which the membrane was clamped was only typically reached within several milliseconds while the time constant of activation for the fast component ranged from 6 to 10 ms, i.e. the recording of the activation phase of the current was partly obtained under a voltage command that was continuously changing (non-stationary level). For the slow component, except for the inactivation time constant, which was slightly reduced in DMD cells, changes in the same direction (slowing down in DMD) were observed. In this case the changes could not be attributed to the higher capacitance and to the subsequent possible slower charging of the membrane as

the kinetics of the slow component of the current were one order of magnitude slower than those of the fast component.

According to their membrane potential dependence, these two types of calcium current could be attributed to T- and L-type components formerly studied in aneurally cultured human myotubes (Rivet *et al.* 1990). While not part of the focus of the present study, a third type of calcium current was also sometimes observed on co-cultured myotubes (not shown). These currents were similar to those observed by Rivet *et al.* (1992) on aneurally cultured myotubes and were present in co-cultured normal (14% of myotubes; $n = 49$) as well as DMD (12% of myotubes; $n = 52$) myotubes. These cells were discarded from the analysis of kinetics and voltage dependence. With regards to the I–V curve of T- and L-type currents, Fig. 3*B* reveals differences in Ca^{2+} current densities between the two kinds (normal and DMD) of cell as well as between $I_{Ca,T}$ and $I_{Ca,L}$. The density of $I_{Ca,L}$ was higher in normal cells than in DMD cells. Measured at +10 mV as the maximum peak amplitude of the global current, the mean value for $I_{Ca,L}$ was significantly (with $P = 0.03$) higher in normal cells (3.9 ± 0.7 pA pF^{-1}; $n = 16$) than in DMD ones (2.0 ± 0.5 pA pF^{-1}; $n = 26$).

In order to characterize $I_{Ca,T}$, nifedipine (5 μM) was used to selectively block $I_{Ca,L}$ as shown in Fig. 4*A*. In the presence of this compound, the current density–voltage relationship (Fig. 4*B*) indicated a maximum peak amplitude for $I_{Ca,T}$ reached with a step potential to −30 mV and a 'zero current' potential near +20 mV in both normal and DMD cells. As for $I_{Ca,L}$, the $I_{Ca,T}$ amplitude was higher in normal (1.39 ± 0.30 pA pF^{-1}; $n = 5$) than in DMD cells (0.90 ± 0.19 pA pF^{-1}; $n = 6$).

In spite of the weak contribution of $I_{Ca,T}$ to the global inward current for high depolarizing steps and the possibility of measuring L-type current amplitude as the amplitude of the whole inward current at high potentials, L-type current could be separated from $I_{Ca,T}$ by holding the membrane potential (V_h) at −50 mV (Fig. 4*C*). Such membrane potential manipulation led to inactivation of $I_{Ca,T}$. In these conditions, a $I_{Ca,L}$ threshold potential of around −30 mV could be observed in both normal and DMD myotubes. More important was the shift of 6–7 mV of the activation part of the I–V curve observed in DMD myotubes towards positive potentials as compared to that of normal cells. Indeed, the maximum amplitude for the normal $I_{Ca,L}$ was between 0 and +10 mV whereas the maximum for DMD cells was at +10 mV. Another observation was the near disappearance of the amplitude difference between normal and DMD myotubes. This point required a more complete approach of the inactivation-dependent process as reported below.

The voltage dependence of calcium current availability (inactivation) has been studied in normal and DMD cells by means of a double pulse protocol as shown in the non-

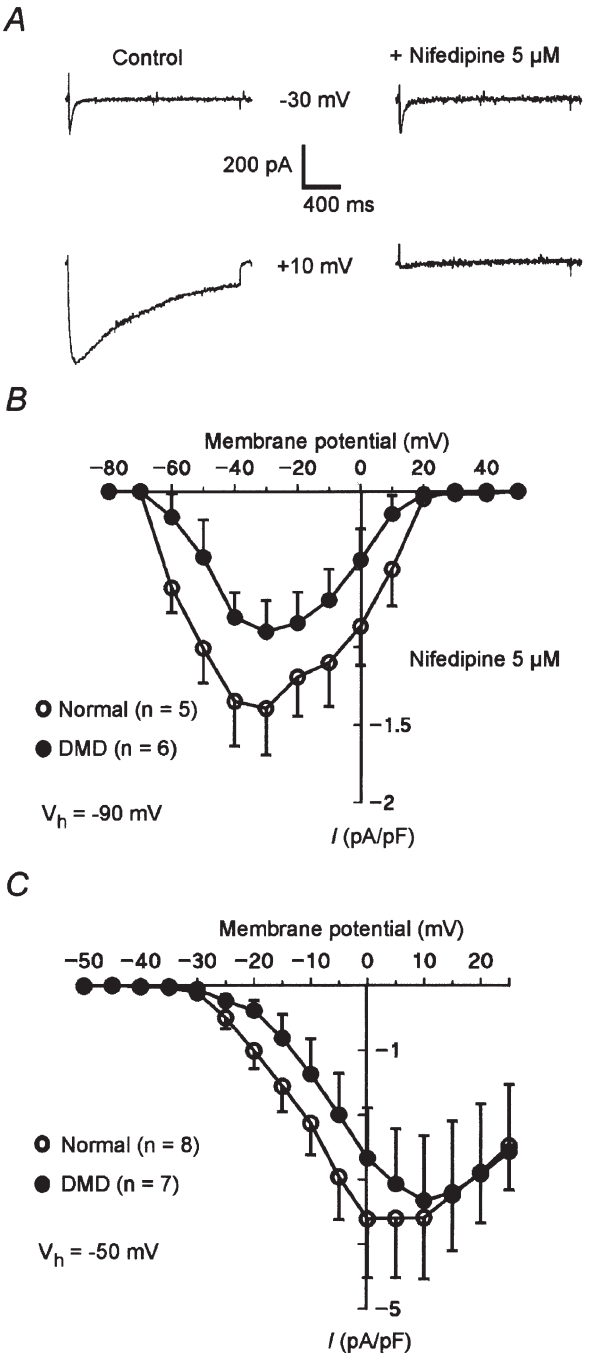

Figure 4. Separation of two types of calcium current in normal and DMD cells

A, examples of calcium currents recorded in control medium (left) and in the presence of 5 μM nifedipine (right) for two depolarizations from a holding potential of −90 mV to −30 and +10 mV. Normal myotubes. *B*, I–V curves obtained in the presence of 5 μM nifedipine in normal (○) and DMD myotubes (●). Holding potential, −90 mV. I is expressed as the peak current density. Values are given as means ± S.E.M. n corresponds to the number of tested cells. *C*, I–V curves obtained as in *B* but in control medium and with a holding potential of −50 mV.

scaled diagrams at the top of Fig. 5*A* and *B*. The steady-state inactivation curves were obtained using a two pulse protocol: 5 s (for $I_{Ca,T}$) or 60 s (for $I_{Ca,L}$) conditioning prepulses (V_{prep}) to different potential levels were followed by a 0.4 s (for $I_{Ca,T}$) or 2 s (for $I_{Ca,L}$) test pulse (V_{test}) to the voltage at which the maximal T-type (−30 mV) or L-type (+10 mV) currents were obtained. Conditioning (prepulse) and test pulses were separated by a 2 or 4 ms return to the holding potential (−90 mV). Steady-state inactivation data were normalized by dividing the current density induced at the test pulse by the maximal amplitude obtained with the most negative conditioning pulse. In order to use all the available data, these were plotted as scatter diagrams. Then, experimental points were fitted by the curve corresponding to a Boltzmann function: $I = I_{max}(1 + \exp(V_{prep} - V_{h,0.5})/k)^{-1}$. $V_{h,0.5}$ (the conditioning potential at which inactivation is half-maximum) and k (the slope factor) were determined for normal and DMD cells. The potential range for $I_{Ca,T}$ inactivation (Fig. 5*A*) in normal cells was around −110 to −40 mV, with $V_{h,0.5}$ of -72.1 ± 0.7 mV and $k = 8.0 \pm 0.6$ mV ($n = 283$, with n corresponding to the number of data points), whereas the potential range for $I_{Ca,T}$ inactivation in DMD was around −100 to −30 mV with a $V_{h,0.5}$ of -61.9 ± 1.4 mV and $k = 8.2 \pm 1.1$ mV ($n = 165$). The 10 mV shift of the inactivation curve of $I_{Ca,T}$ towards more positive potentials in DMD cells, as compared to normal cells, largely exceeded the remaining

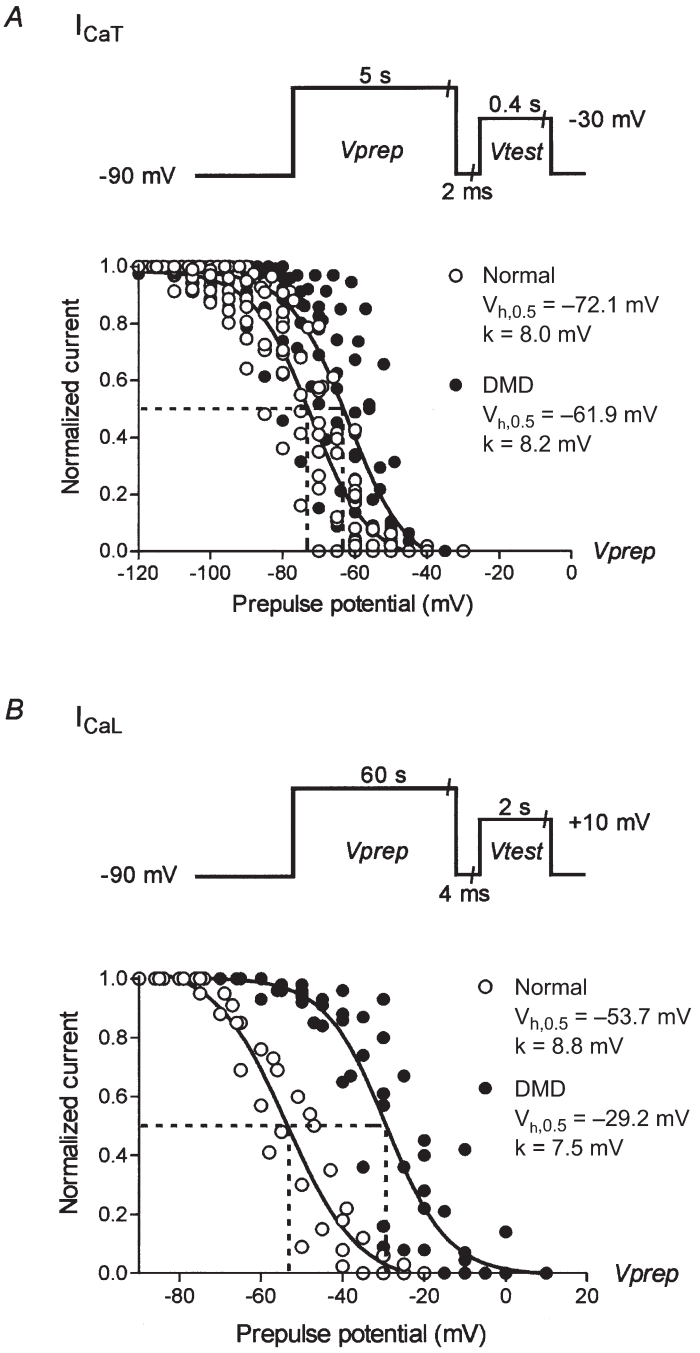

Figure 5. Voltage dependence of the availability of $I_{Ca,T}$ and $I_{Ca,L}$ in normal and DMD co-cultured cells

Steady-state inactivation (availability) curves for $I_{Ca,T}$ (*A*) and $I_{Ca,L}$ (*B*) in normal and DMD myotubes. The potential pulse protocols are shown as diagrams at the top of each panel. The diagrams are not scaled as indicated by interruptions of the lines. The continuous curves were calculated from the Boltzmann function.

voltage drop errors potentially induced by the series resistance (around 1–2 mV, see Methods). Thus, the observed difference between normal and DMD myotubes could be regarded as reliable data resulting from an actual difference between the two kinds of cell. In the same way, but to a larger extent, the $I_{Ca,L}$ inactivation curve in DMD cells (Fig. 5*B*) showed a shift towards more positive values (a 25 mV shift) as compared to that in normal cells, also largely exceeding the voltage drop errors caused by the series resistances, ruling out the possibility that such a difference could be induced by the difference in the amplitude of $I_{Ca,L}$ in normal and DMD myotubes. $V_{h,0.5}$ was -53.7 ± 1.5 mV ($n = 46$) and -29.2 ± 1.4 mV ($n = 76$) in normal and DMD cells, respectively. The corresponding k values were 8.8 ± 1.5 and 7.5 ± 1.3 mV. Hence the inactivation potential range was around -90 to -20 mV and -70 to $+10$ mV for normal and DMD cells, respectively.

Ultrastructural (electron microscopy) data

Normal (control) and DMD co-cultured cells were compared (Fig. 6). In both control and DMD co-cultures there were immature myofibrils developing in the longitudinal axis of the myotubes (Fig. 6*A* and *B*). These initially were composed mostly of actin filaments and dense bodies (Z-line precursors) but, in the more advanced examples, also incorporated myosin filaments such that sarcomeres with separate A-bands, I-bands and Z-lines could be recognized (Fig. 6*B*). In the same micrograph there is a clear Golgi apparatus and vesicles that may be precursors of the sarcotubular system. Numerous caveolae and free vesicles, some of which were fusing, could be observed at the plasma membrane (Fig. 6*C*), and could be precursors of the transverse tubular (T) system. Some sections included profiles of the structures directly involved in excitation–contraction coupling (dyads and triads). Although the sarcoplasmic reticulum (SR) in particular was often ill defined, the characteristic combination of one T-tubule profile and one SR element in a dyad or one T-tubule profile and two SR elements in a triad could be identified (Fig. 6*D*). These structures appeared far rarer in the control than in the DMD co-cultures.

A quantitative technique was used to provide an objective value for the subjective differences observed in the degree of myofibril development in the myotubes. Thus, the sections, each of which covers approximately 100 grid squares (square size, $75\ \mu m \times 75\ \mu m$), were surveyed under the EM and the cells in each alternate grid square were more closely examined. Alternate rather than all grid squares were used because typically a cell profile was very roughly the length of a grid square edge so some crossed the grid bars and were visible in two squares and might have been counted twice. Very few cells crossed two successive bars. The number of cell profiles within a grid square varied from one to seven with a mean of 1.8 for the control and 3.1 for the DMD cultures. This difference seemed to be due to a lower density in the former rather than to a difference in size of the cells. One-hundred grid squares were examined from the DMD cultures and 150 from the controls in order to include comparable numbers of cells. The criterion for including a cell in the counting was that a cell nucleus (or more than one) could clearly be seen. Profiles of cell parts that did not include part of a nucleus were ignored. The cells can be considered as arbitrarily chosen because they are 'selected' by the position in which the sections settle on the grids, which is random with respect to the grid squares. Firstly, the cells were examined for myofibrils. In the profiles of the controls 15.07 % (41 out of 272) cells contained visible myofibrils, and in the DMD cultures 37.9 % (119 out of 314) of cells contained them. This of course does not mean that only 15 or 38 % of the cells contained myofibrils because only very thin sections were examined and a section from a different part of an apparently myofibril-free cell might well reveal them. However, there is a real difference between the two types of cell here. Secondly, the state of differentiation of the myofibrils was examined and a score assigned to each stage. There are three recognizable stages. Stage one: the myofilaments, actin and myosin, are assembled longitudinally but have no transverse alignment, i.e. no bands are visible. The precursors of the Z-bands, the Z-bodies, lie randomly amongst the filaments (score 1.0). Stage two: the Z-bodies align with each other transversely and rudimentary bands can be detected (score 2.0). Stage three: the Z-bodies become narrower and more line-like, and definite A- and I-bands can be detected (score 3.0). Of the 41 control cells with myofibrils, 26 had stage one myofibrils and 15 had stage two myofibrils. This gives a mean score of 1.37 or, if all 272 cells are included, a mean of 0.21. Of the 119 DMD cells with myofibrils, 65 were at stage 1, 51 at stage 2 and 3 at stage 3, giving a mean of 1.48, or 0.56 for the total of 314 cells. Thus the difference in the level of differentiation amongst those cells in which differentiation has been initiated is small, but the proportion of cells in which it has been initiated is notably higher amongst the DMD cells.

DISCUSSION

The main goals of this study were to determine whether differences in calcium movement properties can be observed between normal and DMD skeletal muscle cells co-cultured (contracting) with neuronal explants and whether these differences can in some way be involved in resting intracellular calcium concentration disorders observed in co-cultured DMD cells (Imbert *et al.* 1995, 1996). The present study provides three kinds of data. The first was recordings of the spontaneous variations of transmembrane electrical potential and of free calcium concentration in 'non-stimulated' myotubes. This type of experiment is close to the physiological situation but the derived information about involved mechanisms was more indirect. By contrast the second type of data,

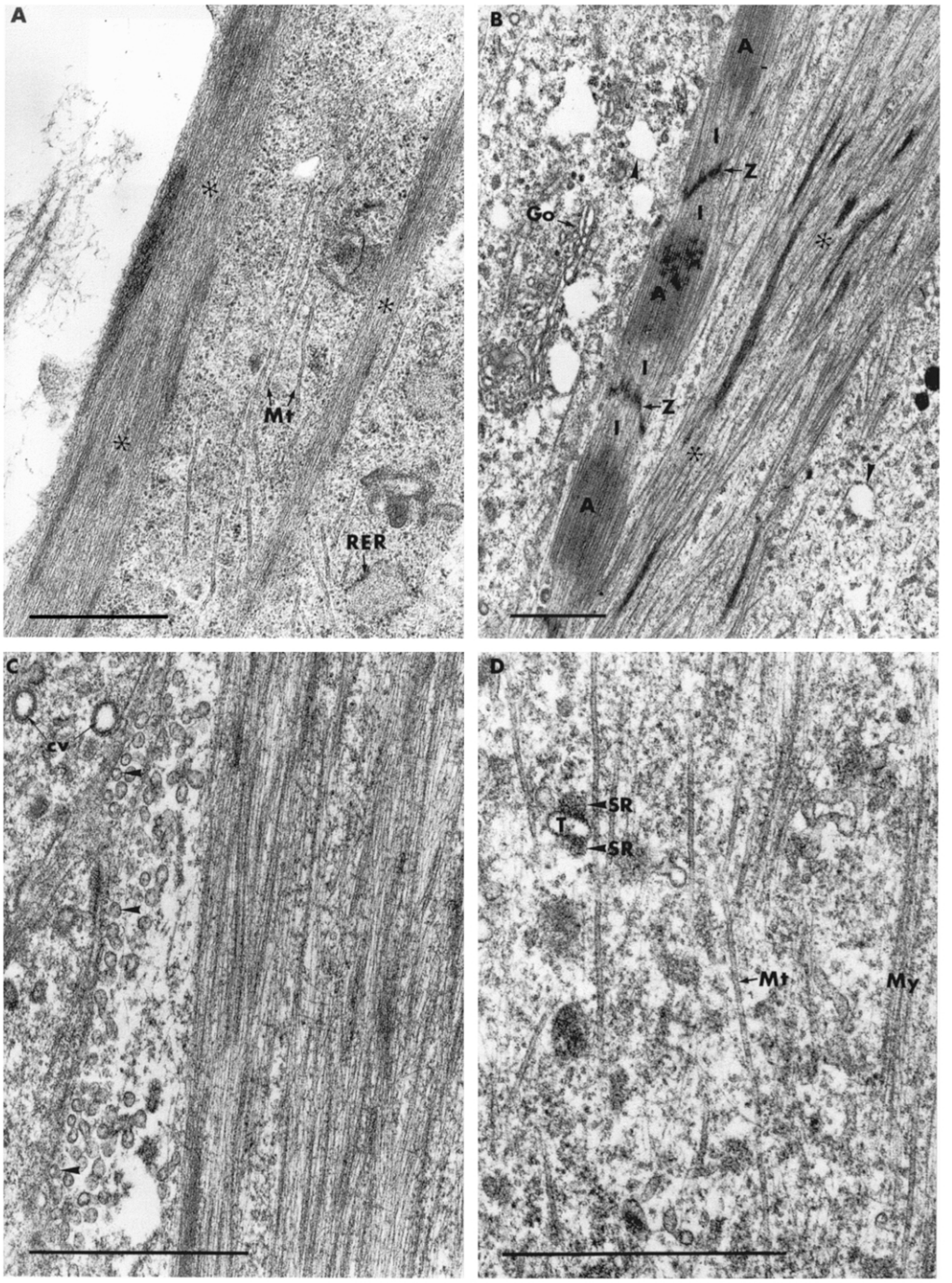

Figure 6. Electron microscopy

A, control. Part of a myotube showing early myofibril development (asterisks). At this stage most of the myofilaments are of actin and there are very few myosin filaments. Microtubules (Mt), rough endoplasmic reticulum (RER) and ribosomes are common. Scale bar = 1.0 μm. *B*, DMD. A myotube showing both early myofibril development (asterisks) and a more advanced myofibril with recognizable sarcomeres containing longitudinally aligned myosin filaments in the A-bands (A). In the same field there is a clear Golgi apparatus (Go) and vesicles (arrowheads) that may be precursors of the sarcotubular system. I, I-band; Z, Z-line. Scale bar = 1.0 μm. *C*, DMD. The edge of a myotube rich in caveolae (arrowheads). Some of these are fusing (or budding) and may be T-tubule precursors. The edge of the adjacent fibre contains coated vesicles (cv). Scale bar = 1.0 μm. *D*, DMD. A myofibril showing an example of early triad formation, although the terminal cisternae of the sarcoplasmic reticulum are not yet well defined. SR, sarcoplasmic reticulum; T, T-tubule; Mt, microtubules; My, myofilaments. Scale bar = 1.0 μm.

obtained in voltage-clamp conditions (patch clamp), provided detailed analysis of the electrical properties of voltage-dependent calcium currents but in ionic and membrane potential conditions quite far from the normal situation. This kind of data needs to be compared with that obtained in the physiological (unclamped) conditions. The third type of data refers to the ultrastructural differences observed between normal and DMD cells.

Spontaneous membrane potential variations and calcium transients

Since the working of calcium channels is closely dependent on variations of membrane potential, the first part of this work was focused on the recording of membrane potential variations at rest and during spontaneous activity. The electrical activity appeared to differ in the two types of cell as follows: in DMD cells, compared with normal cells, (i) the resting potential was slightly less negative (around 4 mV depolarization) and (ii) the AP spontaneous generation frequency was higher (by a factor of around 2.6). V_m of normal cells was similar to that recorded by Saito *et al.* (1990). Since an increase in the absolute value of V_m (more negative membrane potential) seems to accompany the maturation of cells and their degree of innervation (see Saito *et al.* 1990), it could be suggested that the DMD cell development was delayed to some extent compared to that of normal cells. In addition, as expected, a more positive membrane potential appeared to favour AP generation, probably by driving involved ionic channels nearer their activation threshold. With regard to the spontaneous variations of intracellular calcium activity, a similar difference can be observed between the two types of cell with a large enhancement of the spontaneous calcium transients in DMD cells (+45 % as measured by integration).

Calcium current properties: differences between normal and DMD cells

The second set of data deals with the electrical and kinetic properties of T- and L-type calcium currents. The first main result is the smaller current densities of both types of current in DMD cells since the $I_{Ca,L}$ maximum peak density was half that of normal cells, and the $I_{Ca,T}$ corresponding value was 35 % reduced in DMD cells. The other clear result is the overall slow down of the calcium current kinetics in DMD cells. On the basis of the relationship between maturation and calcium current properties observed in rat skeletal muscle by Cognard *et al.* (1993), it could be suggested that DMD cells have a delayed maturation compared to normal cells. This difference between normal and DMD cells was not observed in aneurally cultured human muscle cells (Rivet *et al.* 1990). Another important result is the demonstration of a large difference between the two types of cell at the level of the voltage dependence of $I_{Ca,L}$ inactivation (availability). The strongest evidence of this difference was the large shift (25 mV), in DMD cells, of the $I_{Ca,L}$ inactivation curve on the membrane potential axis towards more positive values. This means that calcium channels remained more available for opening when the membrane potential was driven towards more positive values. For example, at −60 mV nearly all the channels can activate under depolarization in DMD cells while 30 % of them are already in an inactivated state in normal cells. At the physiological level, taking into account the fact that DMD muscle cells present a higher electrical activity (firing), the voltage-dependent properties of the calcium channels described in these cells allow these channels to contribute more significantly to the calcium influx. Nevertheless, as mentioned above, at the same time the calcium current density is reduced in DMD cells. Thus, the overall possible contribution of $I_{Ca,L}$ to the calcium influx remains difficult to evaluate. With regard to $I_{Ca,T}$, the situation appears similar though the inactivation curve shift in DMD cells was considerably smaller (only 10 mV). In addition, due to the very negative potentials at which T-type calcium channels were available, at a physiological membrane potential of −60 mV, for example, only 15 % in normal cells and 40 % in DMD cells of the T-type calcium channels were available for opening. In contrast the remaining fractions of these channels can more easily activate during spontaneous membrane potential variations since their activation threshold is close to the level reached during these variations.

Calcium current properties: comparison with aneural cultures

As compared with that of aneurally cultured cells (Rivet *et al.* 1990, 1992), the voltage dependence of $I_{Ca,L}$ of co-cultured human muscle cells (the present study) appears different, with inactivation curves shifted towards negative potentials as evidenced by the $V_{h,0.5}$ values. A small shift in $V_{h,0.5}$ was also observed for $I_{Ca,T}$ but only in normal co-cultured cells. Another group (Sipos *et al.* 1997; Harasztosi *et al.* 1999) has found more positive values but their data are only derived from normal human cell cultures with high calcium ion concentrations in the bath media (10 mM), which probably led to the well-known charge screening effect and the resulting shift of inactivation curves towards positive values. Thus the co-culture conditions seem to induce a resulting general decrease in the voltage-dependent availability of calcium channels, except for DMD cells where this decrease was significantly stepped down.

Ultrastructure

Contrary to the suggestion from the analysis of calcium current kinetics, the overall picture that emerged is one of a more advanced development of DMD co-cultured cells as compared with normal co-cultured cells, at least for excitation–contraction coupling elements and myofibrils. This is compatible with the observation of a larger capacitance in the DMD cells (despite being a similar size to the normal cells) if this is assumed to be associated with a more fully developed T-tubular membrane system.

Changes in DMD co-cultured human myotubes: a contradictory scheme

Taken together these data do not present a clear scheme for the involvement of calcium channels in the intracellular calcium elevation observed in co-cultured human DMD muscle. On the one hand there are the greater spontaneous membrane depolarizations (resting potential or APs), which would favour the activation of calcium channels, corresponding calcium transient elevations and, possibly, the more advanced cell maturation as evidenced by the ultrastructural observations and the increase in membrane capacitance. On the other hand, in DMD myotubes, the calcium current densities are drastically reduced as is the speed of calcium current activation and inactivation.

Alteration of calcium homeostasis in DMD: several mechanisms involved?

Such a scenario argues more for a general misregulation or destabilization of the calcium channels in DMD rather than an alteration specifically focused on calcium channel proteins themselves. This view is reinforced by the observation that both types of calcium current were altered. Experiments by Imbert *et al.* (1996) and Vandebrouck *et al.* (2001) suggest that other channels and their regulation/expression could be altered in co-cultured DMD muscle cells, in particular cationic channels displaying mechano-sensitive properties. Finally, our present overall hypothesis is that DMD muscle membranes display a general deregulation effect on channel proteins, with a variable level of consequences depending on the particular transmembrane protein affected. In the case of the resting intracellular calcium elevation, the extent of this increase could depend upon the global balance between the different calcium transport mechanisms involved in calcium homeostasis. Following on from this, it remains to be determined to what degree the absence of dystrophin in DMD cells is responsible for such membrane-located alterations.

Bodensteiner, J. B. & Engel, A. G. (1978). Intracellular calcium accumulation in Duchenne dystrophy and other myopathies: a study of 567,000 muscle fibres in 114 biopsies. *Neurology* **28**, 439–446.

Bonilla, E., Samitt, C. E., Miranda, A. F., Hays, A. P., Salviati, G., Dimauro, S., Kunkel, L. M., Hoffman, E. P. & Rowland, L. P. (1988). Duchenne muscular dystrophy: deficiency of dystrophin at the muscle surface. *Cell* **54**, 447–452.

Cognard, C., Constantin, B., Rivet-Bastide, M., Imbert, N., Besse, C. & Raymond, G. (1993). Appearance and evolution of calcium currents and contraction during the early post-fusional stages of rat skeletal muscle cells developing in primary culture. *Development* **117**, 1153–1161.

Delaporte, C., Dautreaux, B. & Fardeau, M. (1986). Human myotube differenciation *in vitro* in different culture conditions. *Biology of the Cell* **57**, 17–22.

Garcia, J., McKinley, K., Appel, S. H. & Stefani, E. (1992). Ca^{2+} current and charge movement in adult single human skeletal muscle fibres. *Journal of Physiology* **454**, 183–196.

Grynkiewicz, G., Poenie, M. & Tsien, R. Y. (1985). A new generation of Ca^{2+} indicators with greatly improved fluorescence properties. *Journal of Biological Chemistry* **260**, 3440–3450.

Hamill, O. P., Marty, A., Neher, E., Sakmann, B. & Sigworth, F. J. (1981). Improved patch clamp techniques for high-resolution current recording from cells and cell-free membrane patches. *Pflügers Archiv* **291**, 85–100.

Harasztosi, Cs., Sipos, I., Kovacs, L. & Melzer, W. (1999). Kinetics of inactivation and restoration from inactivation of L-type calcium current in human myotubes. *Journal of Physiology* **516**, 129–138.

Hoffman, E. P., Brown, R. H. & Kunkel, L. M. (1987). Dystrophin: the protein product of the Duchenne muscular dystrophy locus. *Cell* **51**, 919–928.

Imbert, N., Cognard, C., Duport, G., Guillou, C. & Raymond, G. (1995). Abnormal calcium homeostasis in Duchenne muscular dystrophy myotubes contracting in vitro. *Cell Calcium* **18**, 177–188.

Imbert, N., Vandebrouck, C., Constantin, B., Duport, G., Guillou, C., Cognard, C. & Raymond, G. (1996). Hypoosmotic shocks induce elevation of resting calcium level in Duchenne muscular dystrophy myotubes contracting in vitro. *Neuromuscular Disorders* **6**, 351–360.

Jurkatt-Rott, K., Lehmann-Horn, F., Elbaz, A., Heine, R., Greg, R. G., Hogan, K., Powers, P., Lapie, P., Vale-Sentos, J. M., Weissenbach, J. & Fontaine B. (1994). A calcium channel mutation causing hypokalemic periodic paralysis. *Human Molecular Genetics* **3**, 1415–1419.

Kobayashi, T., Askanas, V. & Engel, W. K. (1987). Human muscle cultured in monolayer and cocultured with fetal rat spinal cord: importance of dorsal root ganglia for achieving successful functional innervation. *Journal of Neuroscience* **7**, 3131–3141.

Maier, F. & Bornemann, A. (1999). Comparison of the muscle fiber diameter and satellite cell frequency in human muscle biopsies. *Muscle and Nerve* **22**, 578–583.

Monnier, N., Procaccio, V., Stieglitz, P. & Lunardi, J. (1997). Malignant-hyperthermia susceptibility is associated with a mutation of the α-1 subunit of the human dihydropyridine-sensitive L-type voltage-dependent calcium channel receptor in skeletal muscle. *American Journal of Human Genetics* **60**, 1316–1325.

Morrill, J. A., Brown, R. H. & Cannon, S. C. (1998). Gating of the L-type Ca channel in human skeletal myotubes: an activation defect caused by the hypokalemic periodic paralysis mutation R528H. *Journal of Neuroscience* **18**, 10320–10334.

Pressmar, J., Brinkmeier, H., Seewald, M. J., Naumann, T. & Rüdel, R. (1994). Intracellular Ca^{2+} concentrations are not elevated in resting cultured muscle from Duchenne (DMD) patients and in MDX mouse muscle fibres. *Pflügers Archiv* **426**, 499–505.

Ptacek, L. J., Tawil, R., Riggs, R. C., Engel, A., Layzer, R. B., Kwiecinski, H., McManis, P. G., Santiago, L., Moore, M., Fouad, G., Bradley, P. & Leppert, M. F. (1994). Dihydropyridine receptor mutations cause hypokalemic periodic paralysis. *Cell* **77**, 863–868.

Rivet, M., Cognard, C., Imbert, N., Rideau, Y., Duport, G. & Raymond, G. (1992). A third type of calcium current in cultured human skeletal muscle cells. *Neuroscience Letters* **138**, 97–102.

Rivet, M., Cognard, C., Rideau, Y., Duport, G. & Raymond, G. (1990). Calcium currents in normal and dystrophic human skeletal muscle cells in culture. *Cell Calcium* **11**, 507–514.

Rivet-Bastide, M., Imbert, N., Cognard, C., Duport, G., Rideau, Y. & Raymond, G. (1993). Changes in cytosolic resting ionized calcium level and in calcium transients during *in vitro* development of normal and Duchenne muscular dystrophy cultured skeletal muscle measured by laser cytofluorimetry using Indo-1. *Cell Calcium* **14**, 563–571.

Saito, K., Kobayashi, T., Askanas, V., Engel, W. K. & Irishawa, K. (1990). Electrical properties of human muscle cultured in monolayer aneurally and co-cultured with fetal rat spinal cord. *Biomedical Research* **11**, 12–28.

Sipos, I., Harasztosi, Cs. & Melzer, W. (1997). L-type calcium current activation in cultured human myotubes. *Journal of Muscle Research and Cell Motility* **18**, 353–367.

Sipos, I., Jurkat-Rott, K., Harasztosi, Cs., Fontaine, B., Kovacs, L., Melzer, W. & Lehmann-Horn, F. (1995). Skeletal muscle DHP receptor mutations alter calcium currents in human hypokalemic periodic paralysis myotubes. *Journal of Physiology* **483**, 299–306.

Vandebrouck, C., Duport, G., Cognard, C. & Raymond, G. (2001). Cationic channels in normal and dystrophic human myotubes. *Neuromuscular Disorders* **11**, 72–79.

Vandebrouck, C., Imbert, N., Duport, G., Cognard, C. & Raymond, G. (1999). The effect of methylprednisolone on intracellular calcium of normal and dystrophic human skeletal muscle cells. *Neuroscience Letters* **269**, 110–114.

Acknowledgements

We are grateful to C. Besse (SIMIS, Poitiers) for technical help and advice in the sample preparation for electron microscopy. This work was supported by Association Française contre les Myopathies, CNRS and The Franco-British Joint Research Programme. M.J.C. is supported by the Wellcome Trust.

Corresponding author

C. Cognard: UMR CNRS/Université de Poitiers 6558, 40 Avenue du Recteur Pineau, F-86022 Poitiers Cedex, France.

Email: christian.cognard@univ-poitiers.fr

Author's present address

N. Imbert: Laboratoire de Biologie Marine et d'Environnement Marin, Université de La Rochelle, La Rochelle, France.